

Ensemble spectral variability study of Active Galactic Nuclei from the XMM-Newton serendipitous source catalogue

R. Serafinelli, F. Vagnetti, R. Middei

Dipartimento di Fisica, Università di Roma “Tor Vergata”, Via della Ricerca Scientifica 1, 00133 Roma, Italy

E-mail: roberto.serafinelli@roma2.infn.it

Abstract. The variability of the X-ray spectra of active galactic nuclei (AGN) usually includes a change of the spectral slope. This has been investigated for a small sample of local AGNs by Sobolewska and Papadakis, who found that slope variations are well correlated with flux variations, and that spectra are typically steeper in the bright phase (*softer when brighter* behaviour). Not much information is available for the spectral variability of high-luminosity AGNs and quasars. In order to investigate this phenomenon, we use data from the XMM-Newton Serendipitous Source Catalogue, Data Release 5, which contains X-ray observations for a large number of active galactic nuclei in a wide luminosity and redshift range, for several different epochs. This allows to perform an ensemble analysis of the spectral variability for a large sample of quasars. We quantify the spectral variability through the *spectral variability parameter* β , defined as the ratio between the change in spectral slope and the corresponding logarithmic flux variation. We find that the spectral variability of quasars has a *softer when brighter* behaviour, similarly to local AGNs.

1. Introduction

Active galactic nuclei are very bright extragalactic objects, located in the dynamical center of their host galaxy, powered by the accretion of matter around a supermassive ($M_{BH} = 10^6$ - $10^9 M_{\odot}$) black hole, along a geometrically thin, optically thick disk. This disk is believed to be responsible for the optical/UV emission, while a hot ($T \simeq 10^8$ - 10^9 K) corona is believed to produce hard X-ray photons by comptonization of the disk photons. This emission is responsible for the observed power-law like spectrum in the X-ray band.

Variability can be a powerful instrument to probe this physical effect, because it can provide information about both shape and physical behaviour of the corona, which are far from being completely understood.

In addition to the study of amplitude variability, it is also interesting to investigate the spectral variability of active galactic nuclei. This feature has already been studied in the optical/UV band by many authors, (e.g. [1-3]) and a *harder when brighter* behaviour of a power-law spectrum $F \propto \nu^{\alpha}$ has been observed. We use the *spectral variability parameter* β introduced in [1], defined as:

$$\beta = \frac{\Delta\alpha}{\Delta \log F}, \quad (1)$$

relating variations in flux and spectral index α .

In the X-ray band the opposite behaviour (*softer when brighter*) has been found for some individual sources (e.g. [4, 5] and more recently [6]). One of the few systematic studies of X-ray spectral variability has been performed by Sobolewska and Papadakis [7], who found such behaviour for 10 nearby Seyfert galaxies, hinting that most of the sources can match the scenario of the superposition of a constant reflection component that overlaps a power-law component, variable in both amplitude and slope.

Currently there have been no systematic studies concerning the spectral variability of quasars and high-luminosity type-1 AGNs, one notable exception being [8], in which the authors find evidence of spectral variability for a fraction of the sources, also with a softer when brighter trend.

The paper is organized as follows: Section 2 describes the data extracted from the archival catalogues, Section 3 describes the relations between the beta parameter and the hardness ratio variations, Section 4 discusses the results of our analysis.

2. The Dataset

We are looking for the *softer when brighter* effect also in type-1 luminous AGNs and quasars.

In order to select this kind of sources, we have cross-matched the XMM-Newton Serendipitous Source Catalogue (XMMSSC-DR5 [9]) with two quasar catalogues from the Sloan Digital Sky Survey, i.e. SDSS-DR7Q [10] and SDSS-DR12Q [11]. These two optical catalogues are complementary and therefore both must be included, so that the catalogue we are going to analyze could be as complete as possible. SDSS-DR7Q lists 105,783 spectroscopically confirmed quasars and SDSS-DR12Q lists 297,301 quasars. Both catalogs do not include active galactic nuclei classes such as Seyfert galaxies, BL Lacertae and type-2 quasars. Therefore, they are well suited for our goal.

XMMSSC-DR5 contains 565,962 observations taken between 2000 and 2013, corresponding to 396,910 unique sources, which means that many sources have been observed more than once. Since we are dealing with variability issues, we required that the sources must be observed multiple times, at least twice. Therefore we only selected sources with multi-epoch observations.

Catalogue	Number of observations	Number of sources
SDSS-DR7Q	/	105,783
SDSS-DR12Q	/	297,301
XMMSSC-DR5	565,962	396,910
Cross-matched catalogue	7,837	2,700

Table 1. Number of observations and sources listed for all the catalogues used in this work.

Both SDSS catalogues and XMM-Newton Serendipitous Source Catalogue list equatorial coordinates α and δ for each observation. We included in our catalogue every XMMSSC observation that lies within 5" from any catalogued source in any of the two SDSS quasar catalogues. In the cases in which we found the same source in both SDSS catalogues, we chose the one contained in SDSS-DR12Q, because it is more recent.

Something that we had to take into account is that not all of the XMMSSC photometric observations are optimal: the quality of the observation is quantified by a parameter of the catalogue, labeled as `SUM_FLAG`. We excluded from our list the worst photometric observations, meaning all observations with `SUM_FLAG` > 2 and we obtained a final catalogue that has 7,837 X-ray observations, corresponding to 2,700 quasar sources.

The number of observations and the number of sources listed in each catalogue are summarized in Table 1.

3. The β Parameter and the Hardness Ratios

We quantify the spectral variability of a source by means of the *spectral variability parameter* β [1], defined by Eq. 1.

In the X-ray band, though, the *photon index* Γ is more commonly adopted, with the power-law spectra described as $n(E) \propto E^{-\Gamma}$. Γ is thus related to α by $\Gamma = -\alpha + 1$; this means that the spectral variability parameter is:

$$\beta = -\frac{\Delta\Gamma}{\Delta\log F}. \quad (2)$$

Unfortunately, the photon index Γ is not available. However, it is related to the *hardness ratio*, and thus it is useful to look for correlations between the hardness ratios and the fluxes of the ensemble set.

3.1. HR-Flux Correlations

Among the many quantities presented, the XMMSSC-DR5 catalogue lists the integrated flux at five different bands, labeled from EP1_FLUX to EP5_FLUX (that we rename as F_1 to F_5 for simplicity), respectively in the bands 0.2-0.5 keV, 0.5-1 keV, 1-2keV, 2-4.5 keV and 4.5-12 keV. XMMSSC-DR5 also lists *hardness ratios* between fluxes in different bands, defined as follows:

$$HR_i = \frac{CR_{i+1} - CR_i}{CR_{i+1} + CR_i}, \quad (3)$$

where CR_i is the countrate in the band i and is related to the flux F_i by the relation

$$F_i = a_i CR_i, \quad (4)$$

with the conversion factors a_i provided by the on-line utility [WebPIMMS](https://heasarc.gsfc.nasa.gov/cgi-bin/Tools/w3pimms/w3pimms.pl)¹.

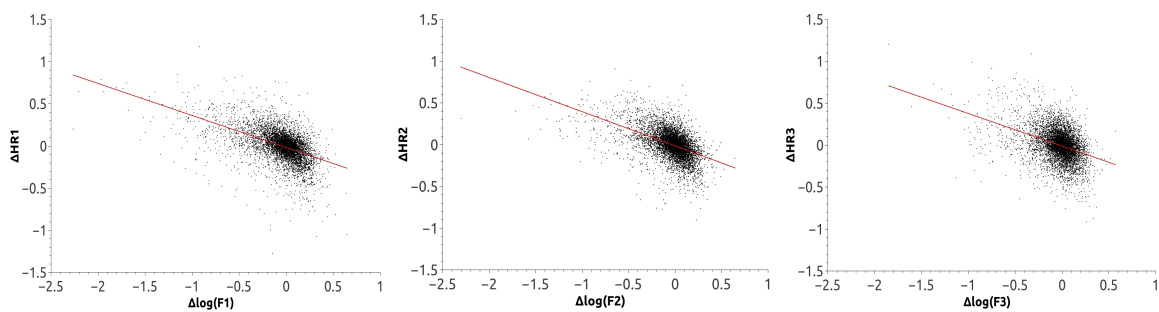


Figure 1. Variations of hardness ratio plotted versus the variations of $\log F$ for the three considered bands. The red line is the least-squares best fit for a linear trend.

We also had to take into account that different sources have different average fluxes and hardness ratios among each other. Thus, instead of correlations between HR_i and $\log F_i$, we studied the

¹ <https://heasarc.gsfc.nasa.gov/cgi-bin/Tools/w3pimms/w3pimms.pl>

Band considered	$\frac{\Delta HR_i}{\Delta \log F_i}$	Correlation coefficient r
ΔHR_1 vs $\Delta \log F_1$	-0.380 ± 0.008	-0.508
ΔHR_2 vs $\Delta \log F_2$	-0.409 ± 0.008	-0.507
ΔHR_3 vs $\Delta \log F_3$	-0.388 ± 0.011	-0.384

Table 2. Slopes and correlation coefficients obtained from ΔHR vs $\Delta \log F$ linear fits.

variations from the mean value of each source of hardness ratio, and the variations, also from the mean value of each source, of the flux logarithm.

We have calculated linear fits for $\Delta HR_{1,2,3}$ vs $\Delta \log F_{1,2,3}$, respectively. Table 2 shows the slopes obtained for each linear fit and the correlation coefficient, while Fig. 1 shows the three fits in the ΔHR_i - $\Delta \log F_i$ planes. The probabilities of finding these correlations by chance are negligible, given the high number of points involved.

3.2. β -HR relation

As we hinted earlier in this section, the spectral variability parameter β can be related to the hardness ratio:

$$\frac{\Delta HR}{\Delta \log F} \simeq \frac{dHR}{d\Gamma} \frac{\Delta \Gamma}{\Delta \log F}.$$

Using Eq. 2 we obtain that

$$\frac{\Delta HR}{\Delta \log F} \simeq -\beta \frac{dHR}{d\Gamma},$$

which means

$$\beta \simeq -\frac{\frac{\Delta HR}{\Delta \log F}}{\frac{dHR}{d\Gamma}}. \quad (5)$$

4. Data Analysis and Results

In order to estimate the spectral variability parameter β we need to consider Eq. 5.

The numerator can be taken from Table 2. It should be stressed that this is an average ensemble estimate, and that the spectral variability behaviour can be different from source to source.

Given the absence of the photon index Γ from our catalogue, we proceeded with simulated data in order to numerically compute the denominator of Eq. 5 as a function of Γ . We have made use of the X-SPEC v.12.9.0 software package [12] to generate some spectral models that could fit our typical sources, using the command `model zwabs*powerlaw`, that also takes redshift into account. According to the standard unified model of AGN [13], type-1 AGNs are unobscured, since they are face-on oriented, which means that the obscuring torus does not affect this kind of active galaxies. One of the spectral models we have considered, therefore, is the unobscured power-law model. Although this is the most likely scenario, one cannot exclude that X-ray obscuration processes are at work, independently from optical/UV obscuration processes. Thus, we have also studied some models that include a moderate absorption over a power-law spectrum. We have only considered models with $\log N_H=21$ and $\log N_H = 22$. We generated models with values of Γ ranging from 1 to 3, the typical values for AGNs, and redshift z between 0 and 3. For each model we have computed the integrated fluxes in bands 0.2-0.5 keV, 0.5-1 keV, 1-2 keV and 2-4.5 keV (or F_1 to F_4 for short), necessary to compute the simulated hardness ratios

HR_1 , HR_2 and HR_3 .

In fact, using Eq. 3 and Eq. 4, and defining $k_i = 1/a_i$, we can write the hardness ratio as:

$$HR_i = \frac{k_{i+1}F_{i+1} - k_iF_i}{k_{i+1}F_{i+1} + k_iF_i}. \quad (6)$$

We were able to compute therefore, for each model, the values of $HR_{1,2,3}$ and the corresponding values of β , by computing the numerical derivatives of HR over Γ .

For typical values of Γ in the range 1-3, this parameter has negative values (see Fig. 2), which means that a *softer when brighter* behaviour is globally present. It is to be stressed that these results extend the trend previously discovered for local sources to a wide redshift and luminosity range.

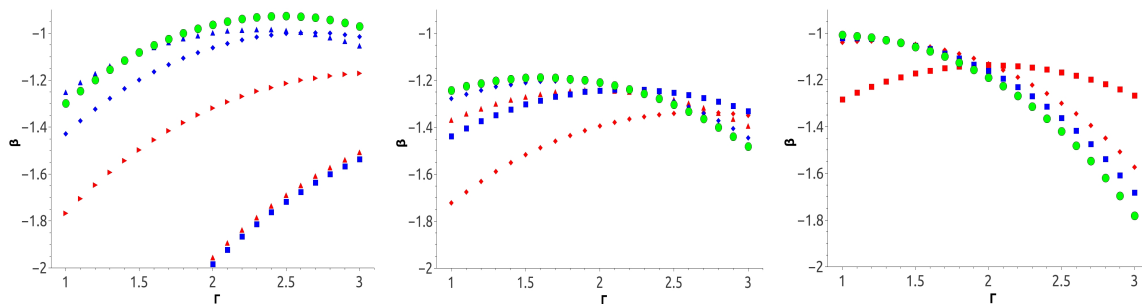


Figure 2. β vs Γ plots for some of the models studied, computed using HR_1-F_1 , HR_2-F_2 and HR_3-F_3 correlations, from left to right. The green circles represent the unabsorbed power-law model, while moderate absorbed power-law models are represented by blue ($\log N_H = 21$) and red ($\log N_H = 22$) symbols. Squares, diamonds, up-pointing triangles and right-pointing triangles refer to redshift $z = 0, 1, 2, 3$ respectively.

Acknowledgements

We thank the organizers of the sixth Young Researchers Meeting. We thank the Gran Sasso Science Institute for their hospitality. This research has made use of data obtained from the 3XMM XMM-Newton serendipitous source catalogue compiled by the 10 institutes of the XMM-Newton Survey Science Centre selected by ESA.

References

- [1] D. Trevese and F. Vagnetti, 2002, *ApJ*, **564**, 624.
- [2] U. Giveon, D. Maoz, S. Kaspi et al., 1999, *MNRAS*, **306**, 637.
- [3] D. E. Vanden Berk, B. C. Wilhite, R. G. Kron et al., 2003, *ApJ*, **601**, 692.
- [4] P. Magdziarz, O. M. Blaes, A. A. Zdziarski et al., 1998, *MNRAS*, **301**, 179.
- [5] A. A. Zdziarski, P. Lubinski, M. Gilfanov, M. Revnivtsev, 2003, *MNRAS*, **342**, 355.
- [6] F. Ursini, P. O. Petrucci, G. Matt et al., 2015, [arXiv:1510.01966](https://arxiv.org/abs/1510.01966).
- [7] M. A. Sobolewska and I. E. Papadakis, 2009, *MNRAS*, **399**, 1597.
- [8] M. Paolillo, E. J. Schreier, R. Giacconi et al., 2004, *ApJ*, **611**, 93.
- [9] S. R. Rosen, N. A. Webb, M. G. Watson et al., 2015, [arXiv:1504.07051](https://arxiv.org/abs/1504.07051).
- [10] D. P. Schneider, G. T. Richards, P. B. Hall et al., 2010, *AJ*, **139**, 2360.
- [11] I. Pâris et al., 2015, in preparation.
- [12] K. A. Arnaud, 1996, *ASP Conf. Series*, **101**, 17.
- [13] R. Antonucci, 1993, *Ann.Rev.Astron.Astrophys.*, **31**, 473.